FARADAY

Coordination of palladium on carbon fibrils as determined by XAFS spectroscopy

Barbara L. Mojet,* Marco S. Hoogenraad, Adrianus J. van Dillen, John W. Geus and Diek C. Koningsberger

Debye Institute, Department of Inorganic Chemistry, Utrecht University, P.O. Box 80083, 3502 TB Utrecht, The Netherlands

To investigate the anchoring of precious metals onto carbon fibrils Pd/C-fibril samples were investigated in both the precursor and the reduced state by X-ray absorption fine structure (XAFS) spectroscopy. Analysis of the XAFS data of the freshly prepared catalyst showed a palladium–tetraamine complex in interaction with carbon. The proposed model involves $[Pd(NH_3)_4]^{2+}$ coordinated to the carbon fibril surface, most probably stabilised by the carboxylic groups (through O—H bridging and charge balance) and the π-electron system of the support. After *in situ* reduction, analysis pointed to small palladium particles of *ca.* 15 Å present on the fibrils with a significant Pd–C interaction.

Introduction

Activated carbon is widely used as an adsorbent and as a support material for catalytically active components in liquid-phase processes because of its high resistance towards strong acidic and alkaline solutions and its high specific surface area. Less favourable are the presence of micropores, which can lead to severe transport limitations, and the liability to attrition; the resulting fines are difficult to separate from the liquid. Carbon fibrils, on the other hand, exhibit a high mechanical strength, contain no micropores, and display a considerable specific surface area and a high pore volume, as determined with nitrogen physisorption.[1,2] It has been shown that precious metals supported on carbon fibrils provide highly active and selective catalysts in hydrogenation reactions.[3] Anchoring on the carbon surface of precious metal precursor compounds as well as precious metal particles obtained by subsequent reduction is difficult owing to the chemical inertness of the surface of carbon fibrils and activated carbon. Drastic pretreatment procedures are therefore required. Studies on amorphous carbon have accordingly revealed that catalyst preparation method and carbon surface chemistry determine the final dispersion of supported precious metals.[4–7] Platinum supported on amorphous carbon was investigated with TEM, XAFS and BET.[4] It was concluded that negatively charged precursor ions do not attach well to an oxidised, negatively charged carbon support surface; however, positively charged complexions can be attached easily.

The observation that the degree of oxidation of the carbon support determines the final metal loading[3] suggests that the number of carboxylic groups is limiting the amount of metal ions that can be attached to the fibrils. Information about the interaction between precious metal compounds and carbon fibrils is therefore very useful for the development of immobilised homogeneous catalysts on carbon.

To investigate the nature of anchoring of palladium precursor ions and palladium metal particles onto carbon fibrils, XAFS experiments were performed on the freshly prepared as well as the reduced catalyst. The results indicate a significant metal–fibril interaction, which accounts for the stabilisation of the precursor complex and the small palladium metal particles obtained after reduction.

Experimental

Catalyst preparation

Carbon fibrils with the graphite layers parallel to the fibre axis were grown in a stream of CO and H_2 out of a 20 wt.% Fe/Al_2O_3 catalyst at 570 °C.[2] Details about the graphitic morphology of the fibrils can be found in the literature.[2,3,8] Reactive species were applied on the fibrils, by treatment with boiling concentrated HNO_3 (65%). The treated fibrils were filtered, washed and dried. Subsequently, the fibrils were (under nitrogen) ion-exchanged with $[Pd(NH_3)_4](NO_3)_2$ and dried at 80 °C. This procedure resulted in a palladium loading of 3 wt.%.

XAFS experiments

The X-ray absorption fine structure (XAFS) spectra were recorded for four samples: Pd-foil, $[Pd(NH_3)_4](NO_3)_2$, ion-exchanged carbon fibrils before reduction {denoted by $[Pd(NH_3)_4]$/C-fibril}, and ion-exchanged carbon fibrils after *in situ* reduction (denoted by Pd/C-fibril). The XAFS experiments were done at the Pd K-edge (24 350 eV) on Wiggler station 9.2 at the SRS Daresbury (UK) using an Si(220) double crystal monochromator {Pd-foil and $[Pd(NH_3)_4](NO_3)_2$} or an Si(220) channel cut monochromator {$[Pd(NH_3)_4]$/C-fibril and Pd/C-fibril}. The double crystal monochromator was detuned to 80% of the maximum intensity at the Pd K-edge. The measurements were performed in transmission mode using ion-chambers filled with krypton to have an absorbance (μx) of 20% in the first and a μx of 80% in the second chamber. All XAFS data were taken at liquid-nitrogen temperature to optimise the signal-to-noise ratio of the spectra.

Sample treatment

All gases were purified and dried before use. The Pd-foil (20 μm) was mounted into a sample holder and placed in an *in situ* cell.[9] $[Pd(NH_3)_4](NO_3)_2$ was thoroughly mixed with BN and an amount with a calculated $\Delta\mu x = 1$ at the Pd K-edge (total absorbance < 2.5) was pressed in a self-supporting wafer and placed in an *in situ* cell. Both Pd-foil and $[Pd(NH_3)_4](NO_3)_2$ were flushed with He at room temperature for 15 min and cooled down to liquid-nitrogen temperature.

Table 1 Parameters of the experimental and theoretical references

backscatterer	reference source	N	R/Å	k-range /Å^{-1}	R-range /Å
Pd	Pd-foil (20 μm)	12	2.75	2.6–21.1	1.99–2.92
N	$[Pd(NH_3)_4](NO_3)_2$	4	2.05	2.8–1.81	0.19–2.54
C	FEFF-3.1[a]	6	4.00		

[a] $S_0^2 = 0.9$, $\Delta\sigma^2 = 0.000$ Å^2.

$[Pd(NH_3)_4]$/C-fibril was pressed into a self-supporting wafer (with a calculated absorbance of 2.5, $\Delta\mu x = 0.4$) and placed in an *in situ* cell. The wafer was flushed with He (purified and dried) at room temperature for 15 min and cooled to liquid nitrogen temperature, where XAFS spectra were collected. The sample was next allowed to warm up to room temperature, and subsequently reduced *in situ* in a flow of 10% H_2 in He at 200 °C (heating rate 2 °C min^{-1}, kept at 200 °C for 1 h) and cooled under He to avoid the formation of palladium hydrides at low temperatures.

XAFS data analysis

The pre-edge was approximated by a modified Victoreen curve[10] and the background was subtracted using cubic spline routines.[11] Spectra were normalised by dividing the absorption intensity by the height of the absorption edge at 50 eV above the edge. The final EXAFS function was obtained by averaging four individual background-subtracted and normalised scans. The XAFS data were analysed in R-space[12] by multiple shell fitting with the data analysis program XDAP.[13] Data for phase shifts and backscattering amplitudes were obtained from reference compounds and FEFF 3.1,[14] the parameters are given in Table 1. Variances for imaginary and absolute parts of the model spectra are calculated by:

$$\text{variance} = 100\% \frac{\int_{R_{min}}^{R_{max}} [k^n(FT_{model}(R) - FT_{exp}(R))]^2}{\int_{R_{min}}^{R_{max}} [k^n FT_{exp}(R)^2]}$$

The errors in the calculated parameters were estimated to be 10% in coordination number N, 1% in distance R, 10% in Debye–Waller factor $\Delta\sigma^2$ and 10% in the inner potential shift ΔE_0.

Results

$[Pd(NH_3)_4]$/C-fibril

The XAFS data of $[Pd(NH_3)_4]$/C-fibril are shown in Fig. 1(a). The data exhibit an excellent signal-to-noise ratio, which makes data analysis possible up to 14.5 Å^{-1}. Examination of the Fourier transforms of $[Pd(NH_3)_4]$/C-fibril and $[Pd(NH_3)_4](NO_3)_2$ [Fig. 1(b), Δk: 3.0–14.5 Å^{-1}, k^{-1}-weighted] reveals differences for both magnitude and imaginary parts of the spectra. In comparison with the spectrum of $[Pd(NH_3)_4](NO_3)_2$, the Fourier transform of $[Pd(NH_3)_4]$/C-fibril shows a somewhat higher intensity and a small shift in imaginary part in the first shell at 1.5 Å, and a significantly enhanced intensity together with a different imaginary part between 3 and 4 Å. Furthermore, the higher shell contribution present in the precursor complex (*at* 5.4 Å) is absent in $[Pd(NH_3)_4]$/C-fibril. Both observations indicate a well dispersed precursor complex in $[Pd(NH_3)_4]$/C-fibril with most probably additional scatterers present, arising from the carbon support surface.

Analysis of the first shell data in R-space [Table 2, Fig. 2(a)] shows a Pd—N contribution at 2.04 Å, which is in accordance with coordination of palladium by four nitrogen atoms as in $[Pd(NH_3)_4]^{2+}$. Inclusion of one or more oxygen atoms in the first shell was investigated to check for the possible existence of a Pd—O interaction in the first coordination shell from the carboxylic groups of the carbon fibril surface. However, these fits did not display the low variances found with only nitrogen as a scatterer. It has been reported previously that it is pos-

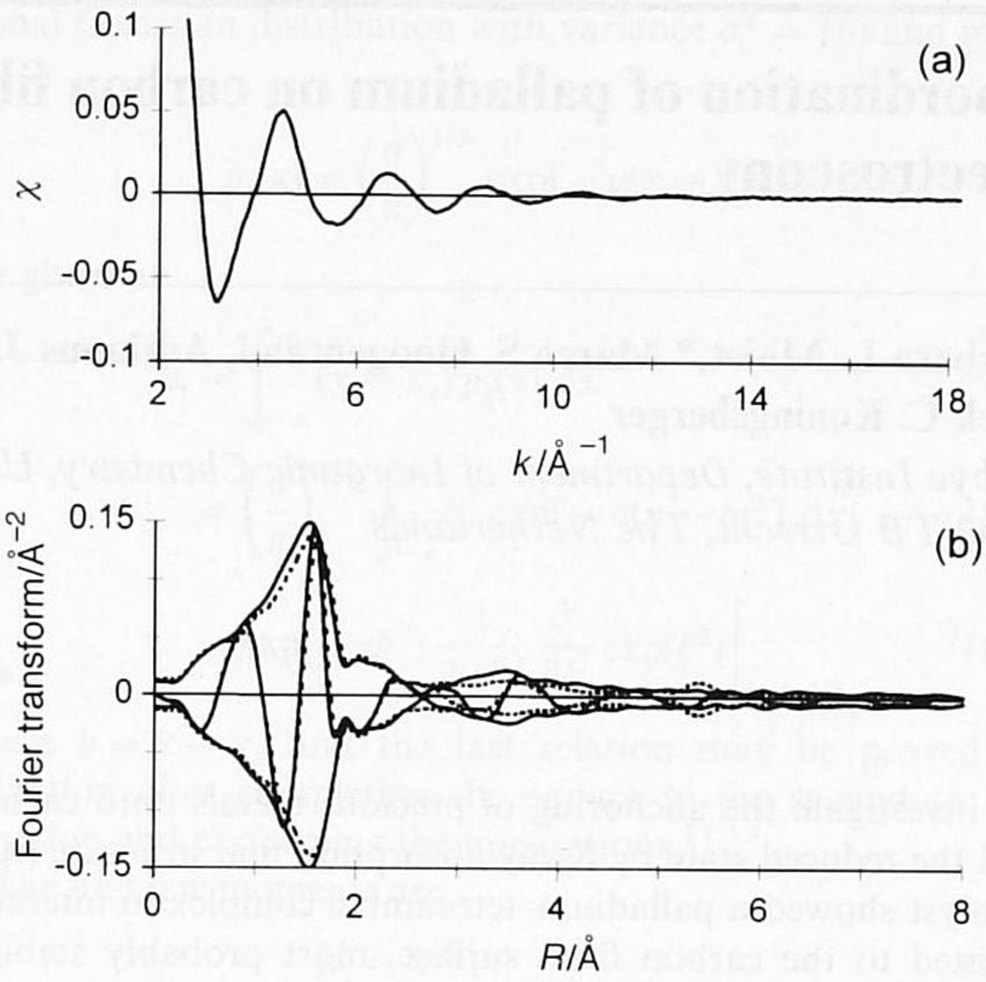

Fig. 1 (a) Raw EXAFS data of $[Pd(NH_3)_4]$/C-fibril. (b) Fourier transform (k^1, Δk: 3.0–14.5 Å^{-1}) of EXAFS data of $[Pd(NH_3)_4]$/C-fibril (solid line) and $[Pd(NH_3)_4](NO_3)_2$ (dashed line).

Table 2 EXAFS analysis parameters and estimated errors for $[Pd(NH_3)_4]$/C-fibril, model I[a]

backscatterer	N	distance/Å	$\Delta\sigma^2/10^{-3}$ Å^2	ΔE_0/eV
N	4.4 ± 0.4	2.04 ± 0.02	− 0.12 ± 0.01	2.2 ± 0.2
C	11.5 ± 1.0	3.95 ± 0.04	17 ± 1	7.7 ± 0.7

[a] R-space fit, k^1 weighting, Δk: 3.00–14.50 Å^{-1}, Δr: 0.50–5.00 Å. Variance imaginary part: 0.36%; variance magnitude: 0.14%.

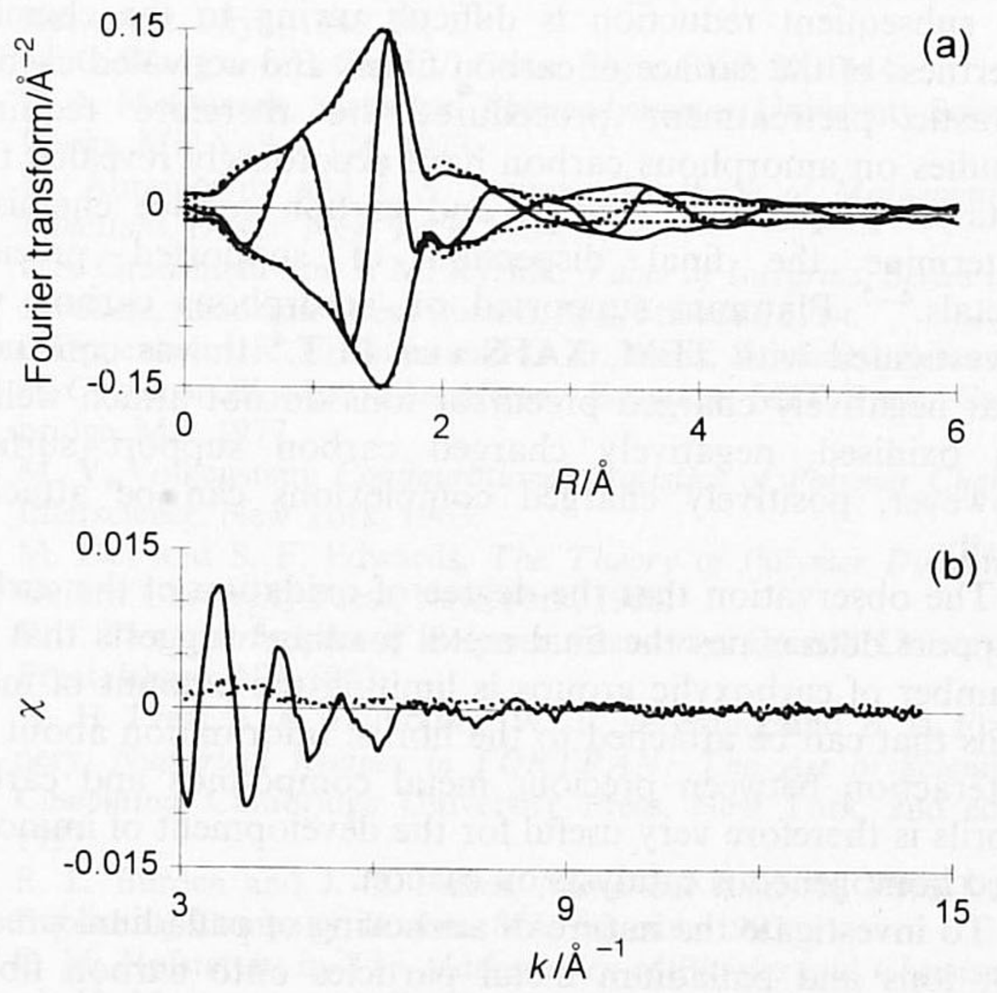

Fig. 2 Comparison of EXAFS data of $[Pd(NH_3)_4]$/C-fibril and calculated first shell (Pd—N). (a) Fourier transform (k^1-weighted, Δk: 3.0–14.5 Å^{-1}) of EXAFS data (solid line) and calculated Pd—N contribution (dashed line). (b) EXAFS data minus calculated Pd—N contribution (solid line) and standard deviation (dashed line).

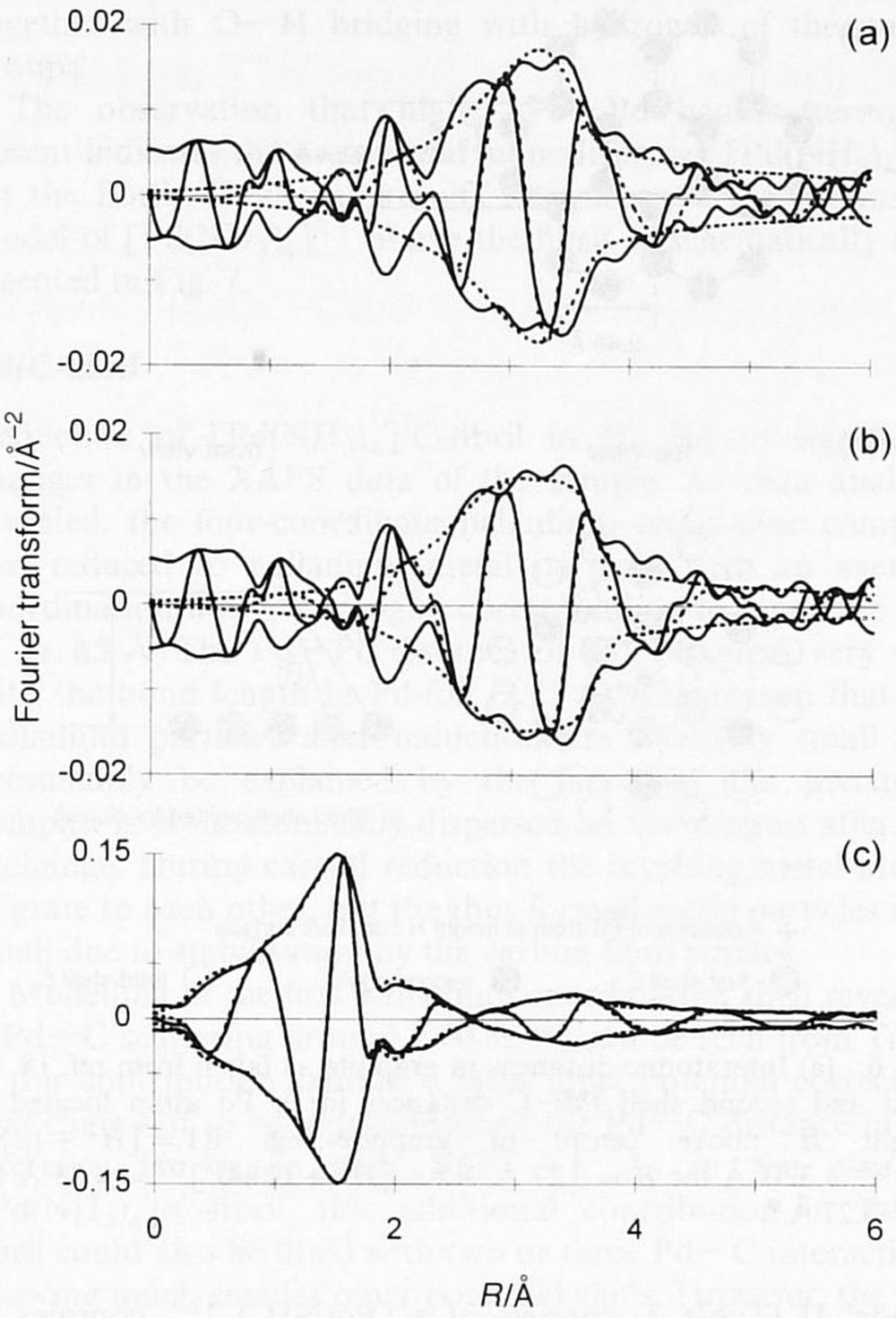

Fig. 3 Fourier transform (k^{-1}-weighted, Δk: 3.0–14.5 Å^{-1}) of EXAFS data of $[Pd(NH_3)_4]$/C-fibril and calculated spectra. (a) Model I: FT of EXAFS data minus calculated Pd—N contribution (solid line) and calculated Pd—C contribution (dashed line). (b) Model II: FT of EXAFS data minus calculated Pd—N contribution (solid line) and calculated Pd—C contributions (dashed line). (c) FT of EXAFS data of $[Pd(NH_3)_4]$/C-fibril (solid line) and calculated spectrum with parameters given in Table 3 (dashed line).

sible indeed to identify N, O and C as different backscatterers, despite the fact that they are neighbouring elements in the Periodic Table.[15]

The difference spectrum of the experimental data of $[Pd(NH_3)_4]$/C-fibril and the calculated Pd—N contribution [Fig. 2(b)] shows that there are significant contributions left above the noise level. This remaining scattering could be successfully fitted with Pd—C scatterer pairs, but determination of coordination numbers turned out to be not straightforward. Fig. 3(a) and (b) show two possibilities (model I and II) for fitting the signal in the Fourier transform after subtraction of the Pd—N contribution from the experimental data. The fit parameters were optimised in a two-shell (model I, 8 free parameters) and three-shell fit (model II, 12 free parameters) and are given in Tables 2 and 3. Model I consists of about twelve carbon atoms at 3.95 Å and model II is the result after refinement with two carbon contributions at 3.57 and 4.30 Å,

Table 3 EXAFS analysis parameters and estimated errors for $[Pd(NH_3)_4]$/C-fibril, model II

back-scatterer	N	distance/Å	$\Delta\sigma^2/10^{-3}$ Å^2	ΔE_0/eV
N	4.3 ± 0.4	2.04 ± 0.02	− 0.34 ± 0.03	1.5 ± 0.1
C	5.9 ± 0.6	3.57 ± 0.03	23 ± 2	− 7.2 ± 0.7
C	6.3 ± 0.6	4.30 ± 0.04	31 ± 3	− 8.5 ± 0.8

R-space fit, k^1 weighting, Δk: 3.00–14.50 Å^{-1}, Δr: 0.50–5.00 Å. Variance imaginary part: 0.35%; variance magnitude: 0.13%.

respectively. The total variances for both models are below 1% as can be seen in Tables 2 and 3. F-tests[16,17] of the fits (including the Pd—N contribution) indicate that both models are equally significant and 90% significant as compared to the model with only Pd—N scattering. The Fourier transforms of the data of $[Pd(NH_3)_4]$/C-fibril and model II are represented in Fig. 3(c). Both magnitude and imaginary parts of experimental data and calculated spectrum are in good agreement.

Pd/C-fibril

Fig. 4(a) shows the Fourier transforms of the XAFS data (Δk: 3.2–14.5 Å^{-1}, k^1-weighted) for $[Pd(NH_3)_4]$/C-fibril and Pd/C-fibril. It is clear that the sample has changed due to reduction in H_2. The contribution at low distance present in the Fourier transform of $[Pd(NH_3)_4]$/C-fibril has vanished and a new peak has appeared around 2.5 Å in the spectrum of Pd/C-fibril. Fig. 4(b) presents the Fourier transforms (Δk: 3.2–15.0 Å^{-1}, k^1-weighted, scaled to 1 on the first Pd—Pd peak) of Pd/C-fibril and Pd-foil. Hardly any higher Pd—Pd shells are visible in the spectra of the catalyst. Differences in imaginary part and magnitude between 1 and 2 Å are clearly indicative for additional contributions. Analysis in R-space revealed besides a Pd—Pd contribution at 2.76 Å also Pd—C scattering at 2.60 Å. Model parameters are presented in Table 4. Comparison of the model spectrum with the experimental data [Fig. 5(a)] and the separate contributions with their difference files [Pd—Pd: Fig. 5(b), Pd—C: Fig. 5(c)] exhibit good agreement for model and experiment in the range 0.5–3.10 Å. At higher distance (R > 3.10 Å) additional contributions are left that are due to higher Pd—Pd and Pd—C shells.

Discussion

$[Pd(NH_3)_4]$/C-fibril

For Pt/C catalysts it has been reported that a significant interaction exists between surface acidic groups and the precursor complex.[4] The authors used XAFS spectroscopy and drew their conclusions by comparing Fourier transforms, without analysing the XAFS data. Since Debye–Waller factors, different types of backscattering neighbours, and coordination numbers determine the shape and intensity of the Fourier transforms, it is difficult to draw conclusions about the coordination sphere of the absorber atoms only from comparison. Analysis of the data analysis is required. In our XAFS data analysis of $[Pd(NH_3)_4]$/C-fibril we found no significant oxygen contribution in the first coordination shell of palladium. Furthermore, an additional scattering between 3 and 4 Å was observed, which was not reported before by others.

This additional scattering could successfully be fitted with Pd—C contributions, although precise coordination numbers were difficult to determine. The uncertainty of the number of coordination shells and neighbours can be attributed to the fact that the carbon support exhibits a very symmetric long range order with multiple carbon–carbon distances. Fig. 6(a) shows the distances in graphite as obtained from literature,[18] that are helpful in the determination of the coordination of the precursor complex to the fibril carbon atoms. Model I (Table 2) corresponds to a $[Pd(NH_3)_4]^{2+}$ complex situated at 3.7 Å above the support with scattering from twelve carbon

Table 4 EXAFS analysis parameters and estimated errors for Pd/C-fibril

backscatterer	N	distance/Å	$\Delta\sigma^2/10^{-3}$ Å^2	ΔE_0/eV
Pd	7.9 ± 0.8	2.76 ± 0.02	3.6 ± 0.3	1.5 ± 0.1
C	7.3 ± 0.7	2.60 ± 0.02	10 ± 1	20.5 ± 2

R-space fit, k^1 weighting, Δk: 3.20–15.00 Å^{-1}, Δr: 0.50–3.10 Å. Variance imaginary part: 0.16%; variance magnitude: 0.08%.

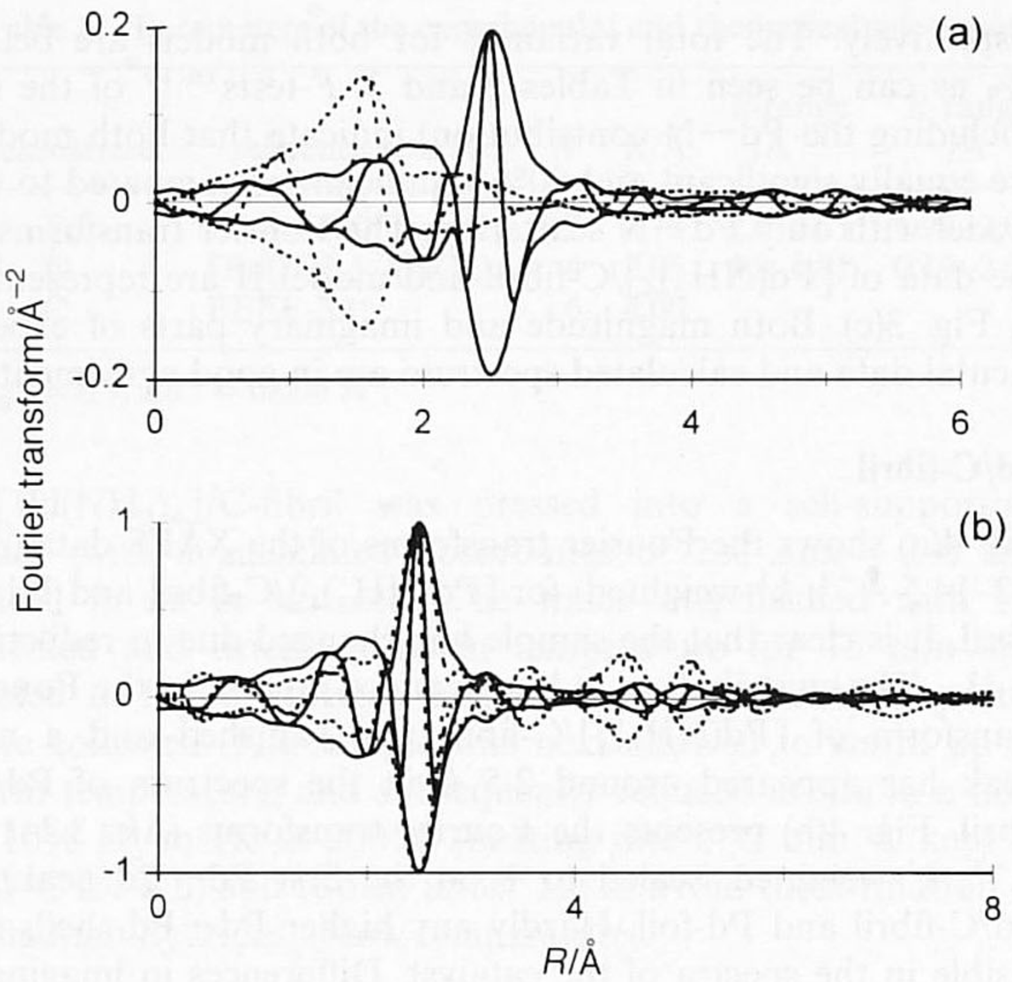

Fig. 4 (a) Fourier transform (k^{-1}, Δk: 3.2–14.5 Å^{-1}) of EXAFS data of Pd/C-fibril (solid line) and $[Pd(NH_3)_4]$/C-fibril (dashed line). (b) Fourier transform (k^1, Δk: 3.2–15.0 Å^{-1}, scaled to 1 on main peak) of EXAFS data of Pd/C-fibril (solid line) and Pd-foil (dashed line).

atoms at an average distance of 3.95 Å. Since the distance between the graphite layers is 3.35 Å,[18] which is about the same in fibrils, it is unlikely that the precursor complex is squeezed between two graphite layers, which could have accounted for a carbon coordination number of twelve. The high coordination number might indicate the presence of several carbon interactions relatively close to each other.

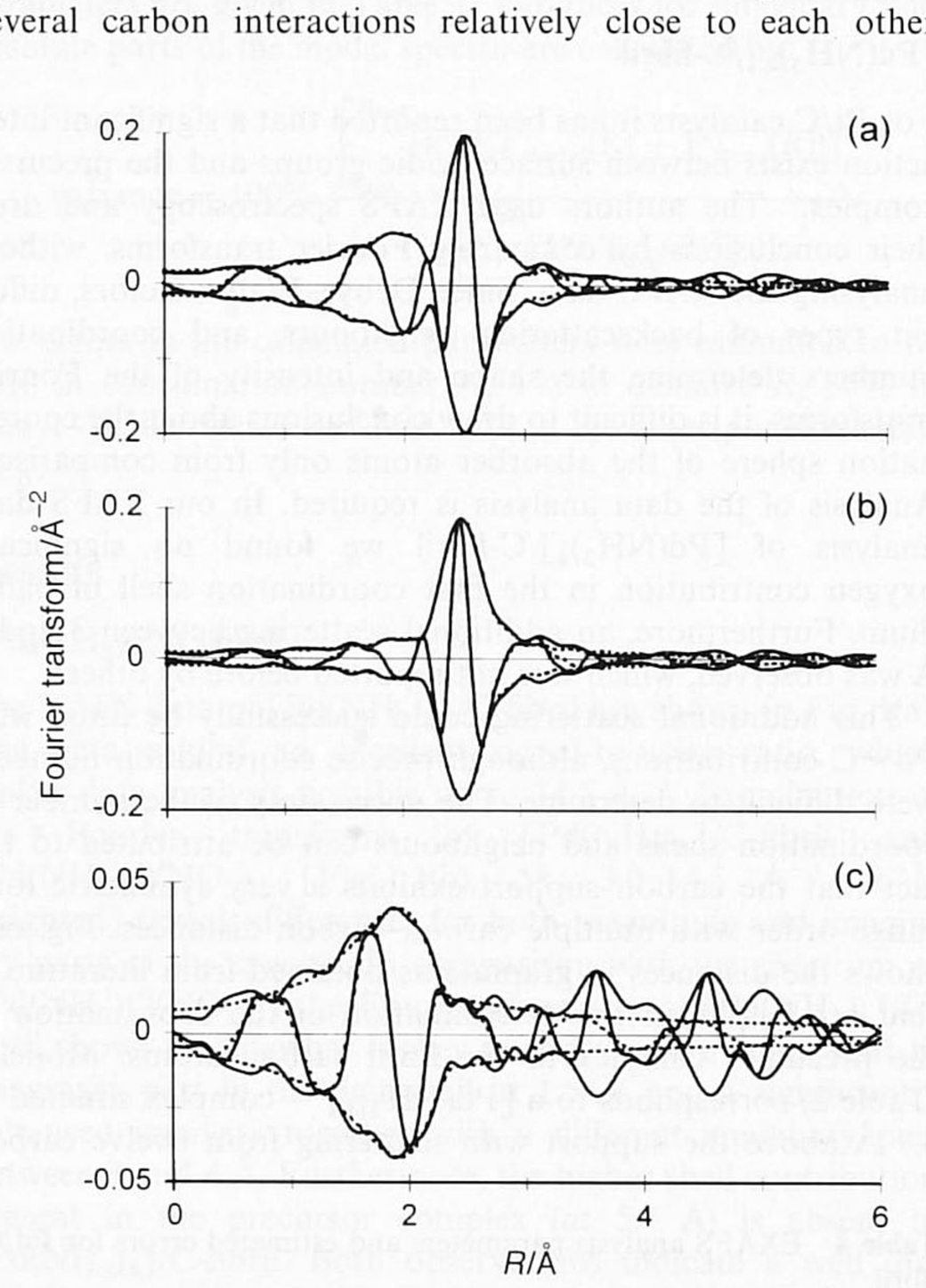

Fig. 5 Fourier transform (k^1 weighted, Δk: 3.2–15.0 Å^{-1}) of EXAFS data of Pd/C-fibril and calculated spectra with parameters given in Table 4. (a) FT of EXAFS data (solid line) and total calculated spectrum (dashed line). (b) FT of EXAFS data minus calculated Pd—C contribution (solid line) and calculated Pd—Pd contribution (dashed line). (c) FT of EXAFS data minus calculated Pd—Pd contribution (solid line) and calculated Pd—C contribution (dashed line).

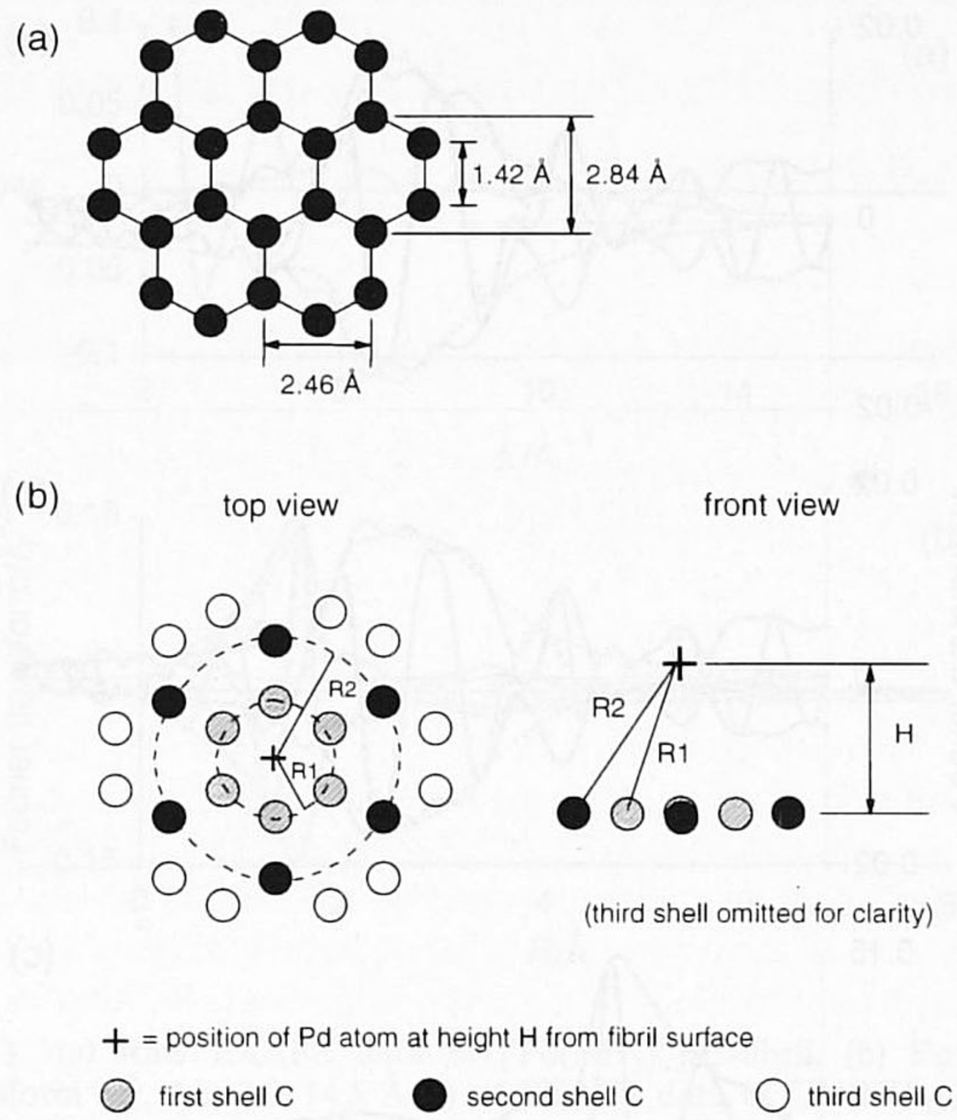

Fig. 6 (a) Interatomic distances in graphite as taken from ref. 18. (b) First and second shell Pd—C distances for a Pd atom located at height H above centre of graphite-ring. R1 = $[H^2 + (2.84/2)^2]^{1/2}$ = 3.57 Å for H = 3.27 Å, R2 = $[H^2 + (2.84)^2]^{1/2}$ = 4.33 Å for H = 3.27 Å.

Model II (Table 3) consists of a $[Pd(NH_3)_4]^{2+}$ complex at 3.27 Å above the fibril, interacting with the first and second six-ring of the carbon system. The Pd—C distances of 3.57 and 4.30 Å are in very good agreement with the distances in graphite [Fig. 6(b)]. In addition, location of the palladium complex at 3.27 Å above the fibril is more likely to give rise to significant support scattering than when it would be at a distance of 3.7 Å which is found in model I. The Debye–Waller factors for the carbon scattering are quite high, but this can be explained by the fact that they are determined relative to a theoretical reference in which $\Delta\sigma^2$ was set to be zero. Furthermore, the precursor complex is located at a relatively large distance from the fibril, which also introduces more disorder as a strong chemical bond is missing. The second Pd—C shell exhibits larger disorder than the first Pd—C shell, which is consistent with higher disorder at larger coordination distances. It was found that models I and II, including Pd—C scattering, result in mathematically good models for the experimental data. Although XAFS spectroscopy alone cannot give unique coordination numbers and distances for the Pd—C interactions in $[Pd(NH_3)_4]$/C-fibril, it shows unambiguously a support–carbon backscattering contribution. Combining mathematics and chemistry suggests model II as the best representative of the geometrical structure of $[Pd(NH_3)_4]$/C-fibril.

In organometallic complexes that contain benzene as a ligand, the metal–carbon distance is around 2.2 Å.[19] Since the observed palladium–carbon distance in this study is much larger, we conclude that no chemical bond exists between palladium and the fibril, although the π-system is likely to have a stabilising effect on the complex.

Although a Pd—O contribution could not be included with statistical significance, oxygen atoms might be present at a longer distance. The immense sea of carbon contributions to the XAFS data might bring about that a few oxygen atoms in a higher coordination sphere of palladium cannot be apparent. As the amount of surface carboxylic groups was found to be important in the preparation of the catalyst,[3,4] but no oxygen could be detected at a short distance from palladium, we suggest a charge stabilising effect of the acidic groups

together with O—H bridging with hydrogen of the amine groups.

The observation that higher Pd—Pd backscattering is absent indicates the presence of monodispersed $[Pd(NH_3)_4]^{2+}$ on the fibrils. Taken all results into account, we propose a model of $[Pd(NH_3)_4]^{2+}$ above the fibril as schematically represented in Fig. 7.

Pd/C-fibril

Reduction of $[Pd(NH_3)_4]$/C-fibril in H_2 led to significant changes in the XAFS data of the sample. As data analysis revealed, the four-coordinate palladium–tetraamine complex was reduced to palladium metal particles with an average coordination number of eight, corresponding to a particle size of *ca.* 15 Å. The Pd—Pd distance of 2.76 Å agrees very well with the bond length in Pd-foil (2.75 Å). The reason that the palladium particles after reduction are relatively small can presumably be explained by the fact that the precursor complex is monoatomically dispersed on the support after ion exchange. During careful reduction the resulting metal atoms migrate to each other, but the thus formed metal particles stay small due to stabilisation by the carbon fibril surface.

Modelling of the first palladium coordination shell revealed a Pd—C scattering around 2.60 Å. As can be seen from Table 4, this contribution exhibits a large inner potential correction that came out to be independent of the Pd—C distance in the reference file made with FEFF-3.1. As in the case of $[Pd(NH_3)_4]$/C-fibril, this additional contribution in Pd/C-fibril could also be fitted with two or three Pd—C interactions showing much smaller inner potential shifts. However, the statistical significance for division of the model into several shells was only 60%.

When the surface of carbon is studied more precisely [Fig. 6(a)], it can be seen that the Pd—Pd distance of 2.76 Å displayed by the reduced catalyst cannot be found in the highly symmetric structure of carbon. This suggests that when a metal particle is attached to a fibril, multiple Pd—C distances at the interface of palladium and carbon exist close to each other, all contributing to the XAFS signal. This can explain the high inner potential shift for the carbon scattering when fitted with only one shell. The average distance of 2.60 Å for the Pd—C interactions points to palladium particles at about 2.2–2.4 Å above the fibril. A similar metal–support distance was also found for platinum metal particles supported on carbon electrodes.[20] The average distance of 2.60 Å is, furthermore, consistent with metal–support distances found in other systems like oxide supported catalysts.[21–23] Fig. 5(b) shows that also scattering at a larger distance (3–3.5 Å) is present. These contributions could be fitted with a Pd—Pd second shell contribution and additional Pd—C scattering, exhibiting large inner potential shifts when fitted with only one contribution. If the metal particles are supported on the fibril, distances around 3 Å and higher indicate the presence of interaction with second carbon shells of the fibrils. Both Pd—Pd and Pd—C coordination numbers and distances as given in Table 4 are consistent with a model of a hemispherical Pd particle of *ca.* 15 Å supported on the fibril. The large π-system of the support and possibly dimples in the carbon surface, due to the oxidation treatment of the fibrils, are likely to account for the stabilisation of the small metal particles obtained after reduction.

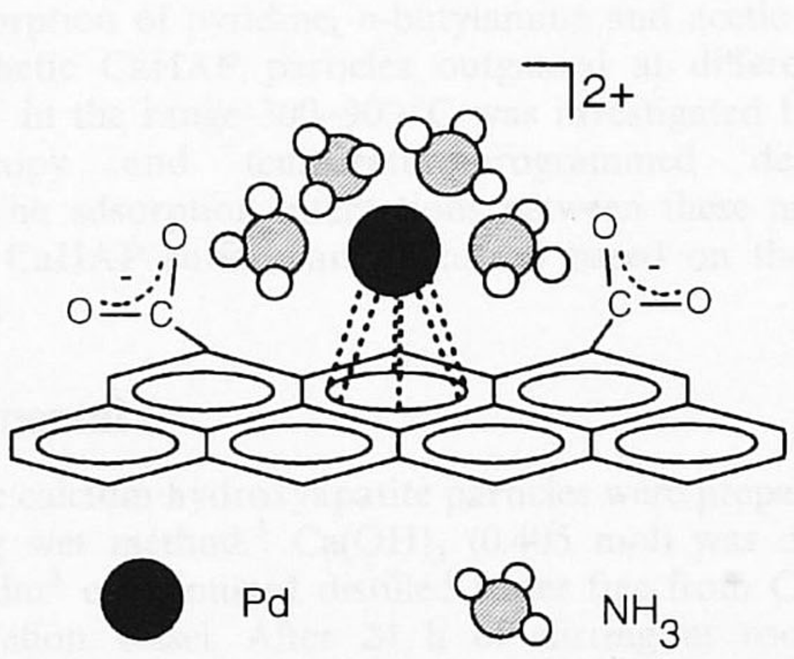

Fig. 7 Schematic representation of proposed structure of $[Pd(NH_3)_4]$/C-fibril

Conclusion

This study showed that no oxygen could be detected in the first coordination shell of palladium after ion-exchange of activated carbon fibrils with $[Pd(NH_3)_4](NO_3)_2$. Furthermore, analysis of the XAFS data revealed a significant metal–fibril interaction for ion-exchanged fibrils both before and after reduction in H_2. The results suggest that a well dispersed precursor complex is stabilised by carboxylic groups on the surface and the π-system of the support. Reduction of this sample results in very small palladium particles in close contact with the support, pointing to an important metal–carbon interaction responsible for anchoring the metal particles to the carbon fibrils.

The authors would like to thank Michel Onwezen and Gijs van Breda Vriesman (Utrecht University) for the preparation of the catalyst, Bob Leliveld (Utrecht University) and Gert van Dorssen (Daresbury Laboratory) for their company and assistance at Daresbury Laboratory.

References

1 N. M. Rodriguez, M. S. Kim and R. T. K. Baker, *J. Phys. Chem.*, 1994, **98**, 13108.
2 M. S. Hoogenraad, R. A. G. M. M. van Leeuwarden, G. J. B. van Breda Vriesman, A. Broersma, A. J. van Dillen and J. W. Geus, *Stud. Surf. Sci. Catal.*, 1995, **91**, 263.
3 M. S. Hoogenraad, PhD Thesis, Utrecht University, 1996.
4 M. C. Román-Martínez, D. Cazorla-Amorós, A. Linares-Solano and C. Salinas-Martínez de Lecea, *Carbon*, 1995, **33**, 3.
5 J. S. Noh and J. A. Schwartz, *Carbon*, 1990, **28**, 675.
6 H. E. van Dan and H. van Bekkum, *J. Catal.*, 1991, **131**, 335.
7 D. J. Suh, T. J. Park and S. K. Ihm, *Carbon*, 1993, **31**, 427.
8 E. Boellaard, P. K. de Bokx, A. J. H. M. Kock and J. W. Geus, *J. Catal.*, 1985, **96**, 481.
9 M. Vaarkamp, B. L. Mojet, M. J. Kappers, J. T. Miller and D. C. Koningsberger, *J. Phys. Chem.*, 1995, **99**, 16067.
10 M. Vaarkamp, I. Dring, R. J. Oldman, E. A. Stern and D. C. Koningsberger, *Phys. Rev. B*, 1994, **50**, 7872.
11 J. W. Cook, Jr. and D. E. Sayers, *J. Appl. Phys.*, 1981, **52**, 5024.
12 K. R. Bauchspiess, *Jpn. J. Appl. Phys.*, 1993, **32**, 131.
13 M. Vaarkamp, J. C. Linders and D. C. Koningsberger, *Physica B*, 1995, **208–209**, 159.
14 J. Mustre de Leon, J. J. Rehr, S. I. Zabinsky and R. C. Albers, *Phys. Rev. B*, 1991, **44**, 4146.
15 K. I. Pandya and D. C. Koningsberger, *Physica B*, 1989, **158**, 386.
16 M. Vaarkamp, PhD Thesis, Eindhoven University of Technology, 1993.
17 D. M. Bates and D. G. Watts, in *Nonlinear Regression Analysis and its Applications*, John Wiley & Sons, New York, 1988.
18 C. L. Mantell, in *Carbon and Graphite Handbook*, John Wiley & Sons, New York, 1968.
19 Ch. Elschenbroich and A. Salzer, in *Organometallics—A Concise Introduction*, VCH, Weinheim, 1989.
20 W. E. O'Grady and D. C. Koningsberger, *J. Phys. Chem.*, in press.
21 M. Vaarkamp, F. S. Modica, J. T. Miller and D. C. Koningsberger, *J. Catal.*, 1993, **144**, 611.
22 D. C. Koningsberger and M. Vaarkamp, *Physica B*, 1995, **209**, 633.
23 M. S. Tzou, B. K. Teo and W. M. H. Sachtler, *J. Catal.*, 1988, **113**, 220.

Paper 7/04989G; *Received* 11*th July*, 1997